

filling of pyrite in the cell lumen of the plant after their initial biodegradation.

The sulphur is an essential element of the soil, which indicates sufficient water supply in the basin. The bacteria available in the sediments do not react fast till oxygen is present. At this stage, fungi and some aerobic bacteria generally degrade organic matter. After the consumption of available oxygen, the anaerobic bacteria, mostly *Thiobacilli*, considerably replace this phase. These *Thiobacilli* are involved in the transformation of sulphate into sulphide during the change-over from oxidizing to reducing conditions. Under anaerobiosis, the sulphide formed from sulphate and organic sulphur compounds may remove iron ions to iron sulphides^{14,19}, but rarely degrade carbohydrates²⁰. The substrate of organic matter provides energy for microbial proliferation during the decomposition of carbonaceous substances and iron is released, which precipitates as insoluble ferric salts. The precipitation thus induces direct action on the organic portion of the compounds, rather than the iron. The high percentage of carbon in degraded leaf cuticles and pyrites indicates the availability of carbon in form of carbohydrates (C₆H₁₂O₆), sugars, etc. It serves a dual function in nutrient supply for both the plants and microorganisms. The biopolymers are transformed through bacterial activity into monomers and other inorganic geopolymers¹⁸. When the degradation of organic matter starts, some compounds quickly disappear, while others (trace elements) which are less susceptible to microbial enzymes persist in the sediments.

Critical observations on the nature and composition of pyrite framboids in freshwater (Mahuadanr) deposits indicate that the framboids were formed in euxinic conditions. Their formation is related mainly to the presence of sulphate-reducing bacteria under the prevalence of reducing conditions in the basin of deposition. The main requisite for the formation of pyrite framboids is a reducing condition and not the location of depositional site under continental or marine realm.

1. Love, L. G., Al-Kaisy, A. T. H. and Brockley, H., *J. Sediment. Petrol.*, 1984, **54**, 869–876.
2. Love, L. G., *Studies in Earth Sciences* (eds Murty, T. V. V. G. R. K. and Rao, S. S.), Today and Tomorrow Printers, New Delhi, 1971, pp. 434–464.
3. Kortenski, J. and Kostova, I., *Int. J. Coal Geol.*, 1996, **29**, 273–290.
4. Renton, J. J. and Bird, D. S., *Int. J. Coal Geol.*, 1991, **17**, 21–50.
5. Lyon, S. P. C., Whelan, J. F. and Dulong, F., *Int. J. Coal Geol.*, 1989, **12**, 329–348.
6. Scheihing, M. H. *et al.*, *J. Sediment. Petrol.*, 1978, **48**, 723–732.
7. Chaiffetz, M. S., *Palynologia*, 1978, **1**, 121–135.
8. Wignall, P. B. and Newton, R., *Am. J. Sci.*, 1998, **298**, 532–552.
9. Kumar, M. *et al.*, *J. Geol. Soc. India*, 2000, **55**, 317–325.
10. Maheshwari, H. K. and Bajpai, U., *Palaeobotanist*, 1997, **46**, 31–34.
11. Taeglaar *et al.*, *Palaeobiology*, 1991, **17**, 133–144.
12. Leban, C., *Phytopathology*, 1988, **78**, 179–185.

13. Andrew, J. A. and Hirono, S. S., *Microbial Ecology of Leaves*, Springer-Verlag, New York, 1991, p. 499.
14. Alexander, M., *Introduction to Soil Microbiology*, John Wiley and Sons, New York, 1977, p. 467.
15. Tucker, M., *Techniques in Sedimentology*, Blackwell Scientific Publications, Oxford, 1988.
16. Berner, R. A. and Raiswell, R., *Geology*, 1984, **12**, 365–368.
17. Agarwala, S. C. and Hewitt, E. J., *J. Hart. Sci.*, 1954, **29**, 291.
18. Berner, R. A., *Early Diagenesis*, Princeton University Press, New Jersey, 1980, p. 241.
19. Staley, J. T., Bryant, M. P., Pfennig, N. and Holt, J. G., *Bergey's Manual of Systematic Bacteriology*, Williams and Wilkins, Baltimore, 1989, vol. III, pp. 1601–2298.
20. Kreig, N. R. and Holt, J. G., *Bergey's Manual of Systematic Bacteriology*, Williams and Wilkins, Baltimore, 1989, vol. I, pp. 1–964.

ACKNOWLEDGEMENT. We thank the Director, Birbal Sahni Institute of Palaeobotany for providing infrastructural facilities during the course of present study.

Received 21 August 2000; revised accepted 7 March 2001

A new approach to the analysis of transverse river valley profiles and implications for morphotectonics: A case study in Rajasthan

S. Sinha-Roy

Birla Institute of Scientific Research, Statue Circle, Jaipur 302 001, India

Study of river profiles provides significant information on both hydrodynamic factors and geomorphic features of drainage basins. Longitudinal river profiles have been extensively studied and different parameters have been proposed by various authors for these profiles, but transverse river valley profiles (TRPs) have not received similar attention. A new approach to the TRP analysis has been proposed here. It identifies several TRP parameters that are easily quantifiable. These quantified parameters are useful for inter-TRP and as well as inter-drainage basin comparisons. These are also useful to derive drainage basin attributes such as valley symmetry and the state of valley erosion, identify and correlate geomorphic features such as plantation surfaces, and importantly, to draw morphotectonic inferences. The procedure has been successfully tested in a case study of the Banas drainage basin, Rajasthan.

GEOMORPHOLOGISTS study two types of river valley profiles to assess drainage basin evolution and to draw inferences on geologic controls as well as on morphotectonics.

e-mail: ssinharoy@yahoo.com

The most commonly analysed are the longitudinal river profiles whose quantified parameters are used to compare different drainage systems, and specifically, to identify the response of neotectonic activities in the drainage basins¹⁻⁴. On the contrary, the transverse river valley profiles (TRPs) have not received much attention, except that these are generally used to ascertain the valley symmetry⁵ and attempt pediment or river terrace correlation⁶⁻⁸. This communication describes a new approach to define and analyse several parameters of TRP and gives an example of their usefulness in drawing morphotectonic inferences from a case study of the Banas drainage basin, Rajasthan.

The conventional TRP across drainage basins has several drawbacks. First, such TRPs are difficult to use to compare different TRPs across the same basin and also those across different basins, because of variable valley elevations and profile lengths. Secondly, the shape of such TRPs is scale-dependent, and hence, fixing of horizontal and vertical scales of the TRPs, particularly for the long ones across basins having highly contrasting altimetric, frequency is problematic and subjective. These aspects restrict the usefulness of the conventional TRPs. These problems can be circumvented to a large extent by normalizing the two variables, namely the elevation and the distance.

Figure 1 shows the normalized TRP of a hypothetical river valley cross-section where the breaks in the curve slope are taken to represent terraces (*Ts*), although these breaks could also represent pediments, planation surfaces and lithologic contrasts. The abscissa is L_i/L , where L is the profile length and L_i is the distance of the individual data points from the valley summit or watershed on one end of the profile. The ordinate represents $\Delta H_i/\Delta H$, where ΔH is the difference between the maximum and the

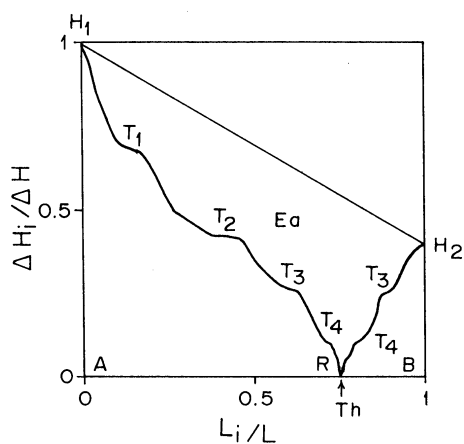


Figure 1. Normalized transverse river valley profile (TRP) across a hypothetical river valley. $\Delta H_i/\Delta H$ is the individual height data (H_i) normalized against the maximum and the minimum height differential (ΔH), L_i/L is the individual data-point distance (L_i) from one end of TRP normalized against total TRP length (L). Th , Thalweg of the main river; T_1 – T_4 , Terrace positions; H_1 , H_2 , Valley top on the left and right banks, respectively; Ea , Measure of valley erosion. For explanation see the text.

minimum elevations of the profile, ΔH_i is the difference in the elevation between the individual data points and the maximum elevation of the profile. Both L_i/L and $\Delta H_i/\Delta H$ vary between 0 and 1, and thus allow for easy comparison of the parameters of different TRPs. The thalweg (Th) of the main river, being located at the minimum height in the TRP, would plot (R) on L_i/L axis at $\Delta H_i/\Delta H = 0$, while the tributary confluences can be shown on the profile curve. The area (Ea) between the profile curve and the line H_1 – H_2 joining the two points of the watershed summits on opposite sides of the valley, expressed as per cent of the area ABH_2H_1 , is an approximate 2D measure of the total valley erosion in the given TRP.

The shape of TRP curves reflects the extent of the valley erosion, which depends on many factors, among which the duration of erosion, the bedrock resistance and neotectonic activity causing terrane uplift and subsidence are important. Figure 2 shows the smoothed TRP curve, where Th – M join (Ch) is a measure of the maximum vertical incision at the current channel site. The value of Ch does not necessarily give the extent of the valley-side incision, because the valley-side shape is controlled also by other non-hydrological factors unrelated to the main river channel, assuming that the latter has not shifted its position drastically across the valley. Some of these factors are erosion by the tributaries and masswasting at the valley-sides. In order to assess the role of these factors, it is necessary to define the TRP curve shape away from the present river channel in terms of its concavity. As the valley-side shape is also linked with the position and the elevation of the present channel which is the local base-level of erosion, the point M on H_1 – H_2 line is joined with the point A , depicting the main channel elevation. The line intersects the TRP curve at the point P . P – N is the normalized expression of average valley-side incision (Eh). Each TRP has two values of Eh , one for the left bank [$Eh(L_B)$] and the other for the right [$Eh(R_B)$]. Eh/Ch ratio indicates the relative significance of factors other

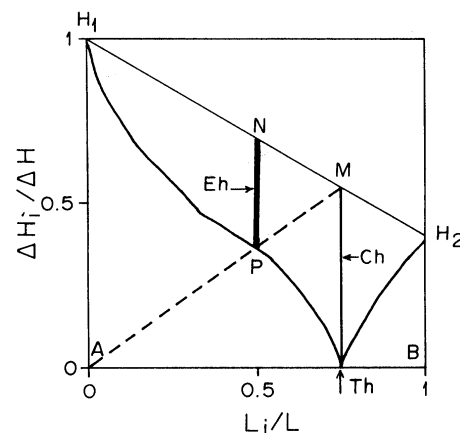


Figure 2. Smoothed hypothetical TRP curve from which Eh and Ch are extracted for one valley side. Th , Thalweg of the main river. For explanation see the text.

than erosion by the main river, especially tributary erosion on the valley-side slopes. The higher the ratio, more significant is the role of tributary and masswasting in valley-side erosion. On the other hand, this ratio tends to decrease in cases where the incision along the main river channel is high due to, for example, rejuvenation.

The drainage basin symmetry with respect to the main river channel has two connotations. First, theoretically the basin should be symmetric such that the catchment areas on both banks of the river are equal or nearly equal. Generally, however, drainage basins are asymmetric, a feature caused by inherent heterogeneity in the boundary conditions of the catchment area, the initial position of the channel with respect to the valley flanks, or in some cases, by the water-divide migration consequent upon river piracy⁹. High degree of headward erosion by the river system on one basin might result in the capture of a part of the catchment area of the adjacent basin due to neotectonic movements¹⁰. Second, the difference in the slopes of the two valley sides causes the valley asymmetry for which geologic, hydrologic and climatic factors are responsible^{5,11,12}. Figure 3 shows a method to quantify these two symmetry parameters. The basin symmetry (B_s) is given by $AT - 0.5$, where AT is the normalized distance of the thalweg from one end of the profile, 0.5 is the midpoint of the TRP on L_i/L axis which is the central point of the drainage basin on the profile. B_s values would vary from +0.5 to -0.5, with zero value indicating perfectly symmetric basin. The gradient of the valley sides on either bank is not uniform, and hence, the lines joining H_1-T and H_2-T do not give the average slope on the left bank and the right bank, respectively. In order to obtain a more realistic measure of the valley-side slope (V_s) from TRP, the form surfaces of the TRP curves are obtained by joining the maximum deflection points on the concave and convex sides of the profile curves for each bank with T , the thalweg (broken lines in Figure 3). The form surface angles for both LB and RB curves are bisected. The angles between the bisectors and the line TM give the V_s values.

It may be noted that the valley-side slopes (V_s) thus computed do not give the actual valley-side slope angle. The difference in the V_s values for the left bank and the right bank is a measure of the valley symmetry (V_a). The lower the V_a value, the higher is the valley symmetry. V_s may be related to Eh and Ea because flatter valley-side slopes (high V_s) would indicate greater degree of incision. On the contrary, B_s cannot be linked with any other TRP parameter, but it has a bearing on the influence of geomorphic features (tributary confluence, terrace dispositions, river capture, etc.), geological aspects (lithologic contacts, neotectonic features, etc.) and other boundary conditions of the drainage basin.

The degree of valley erosion is not uniform along the length of the main river, and hence, Ea and Eh values of the TRPs across different segments of the drainage basin

would vary. In order to compare the degree of erosion at different TRP locations, the parameter $Eh * \mathcal{L}_n$ is useful. (\mathcal{L}_n is the normalized profile length derived from the ratio L_p/L_{max} , where L_p is the length of the individual TRP, i.e. the valley width at each TRP location, L_{max} is the maximum length of the study TRPs, generally the maximum valley width, Eh^* is the mean Eh value of the given TRP). $Eh * \mathcal{L}_n$ is an important parameter for expressing valley incision on two counts. First, it is a 2D parameter, and secondly, it incorporates an element of linkage through \mathcal{L}_n between all the study TRPs of the basin. On both these counts $Eh * \mathcal{L}_n$ parameter is better than Eh used alone for TRP comparison. Generally, $Eh * \mathcal{L}_n$ is influenced largely by non-hydrologic factors. For example, higher value of this parameter would indicate greater valley erosion in response to either neotectonically controlled uplift of blocks or the presence of easily erodible bedrocks. A similar parameter using the actual valley side-slope elevations instead of normalized values in longitudinal river profiles has been used to obtain the approximate bedload/discharge ratios that are large in highly-eroded valleys^{4,13}.

One of the important geomorphic features that the TRPs are capable of highlighting is the planation surfaces (pediment, river terrace, piedmont, etc.). The continuity of a given surface along the river valley and an associated tendency for the surface remnants to generally occur at uniform heights above the present stream is a primary criterion for their correlation⁵. The relative elevations of the surface sets are also an important basis of correlation¹⁴. Reconstruction and correlation of planation surfaces in different TRPs are better achieved in normalized profiles than in conventional cross-sections. The procedure would be to identify the planation surfaces from the shape of and the slope breaks in TRP curves, and after field checks, to convert their $\Delta H_i/\Delta H$ values to actual

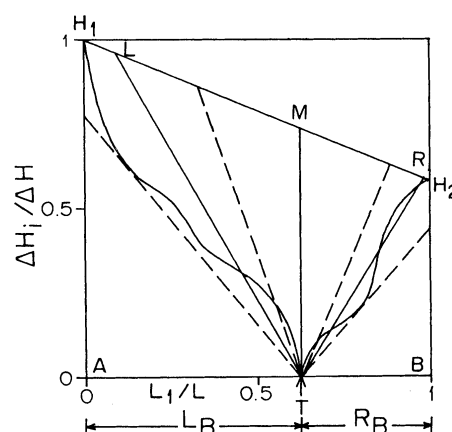


Figure 3. Method of computation of basin symmetry (B_s) and valley symmetry (V_a). Dotted lines are form surfaces of profile curves originating from T (thalweg of the main river). The angles between the bisectors of the form surface angles at T and the line TM give the generalized valley slope on each valley side. This is not the actual gradient but $\angle LTM - \angle RTM$ gives the valley symmetry (V_a) and $AT - 0.5$ gives the basin symmetry (B_s). L_B , Left bank; R_B , Right bank.

heights (HT). The minimum height in the profiles, generally the elevation of the thalweg of the main river, is deducted from all HT values to obtain ΔH_i value for the individual planation surfaces which is then normalized with respect to ΔHP (difference between the maximum and the minimum elevations among the study TRPs). The surfaces are plotted against the individual TRPs from which their relative dispositions with respect to one another and also to the main river channel become clear for regional correlation and interpretation.

An example of the TRP analysis following the procedure outlined above is given here as a case study in the Banas drainage basin, Rajasthan (Figure 4). The Banas, a 6th order Hortonian river, is the longest (510 km) in Rajasthan, and has a basin area of ca. 46,660 sq km. The basin is delimited in the NW by the Aravalli hill range and in the SE by the Vindhyan plateau. Three TRPs ($A-B$ to $E-F$) across the basin have been studied (Figure 4). It may be noted that for such studies to be meaningful, it is necessary that the profile lines are orthogonal to the trend of the main river channel in narrow valleys and/or to the axis of wide valleys within which the main river may meander. The study TRPs along $E-F$ and $C-D$ are nearly orthogonal to both the general trend of the Banas channel and the valley axis, while the TRP: $A-B$ is slightly oblique to the general channel trend, but is orthogonal to the valley axis which in the SW segment of the basin is almost E-W. The non-parallelism of the general trend of the channel and the valley axis is because of the asymmetric nature of the Banas drainage basin¹⁰, and also due to

the fact that the asymmetric Banas valley is wide and relatively flat at the base. The Banas drainage basin shape and the water-divide outline do not indicate the valley axis orientation, especially in the SW segment. The normalized TRPs are shown in Figure 5. The different parameters defined above, are computed for these TRPs (Table 1). The TRPs show the position of the river terraces (T), pediment surfaces (P), and also the probable faults (F), identified from the slope variations and the breaks in the TRP curves. Normalized terrace positions are shown in Figure 6.

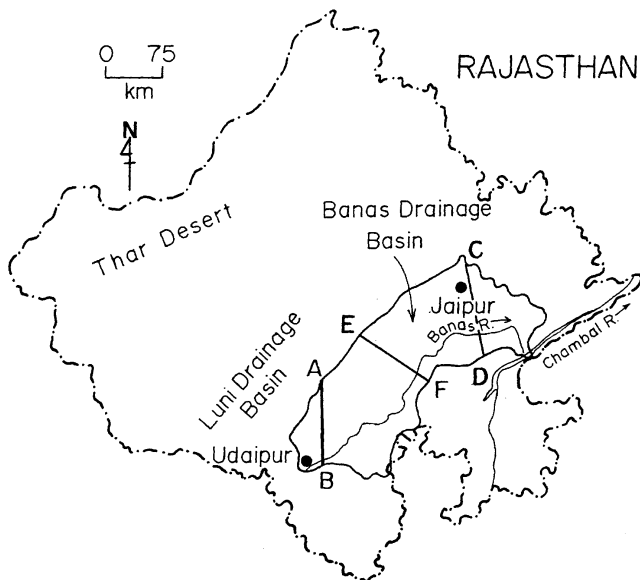


Figure 4. Location of the Banas drainage basin in Rajasthan showing the position of the analysed TRPs ($A-B$, $C-D$, $E-F$). The profile locations are so chosen that these represent the upper, middle and lower reaches of the Banas drainage basin. Note the drainage basin asymmetry due to larger catchment area on the left bank than on the right bank of the Banas river.

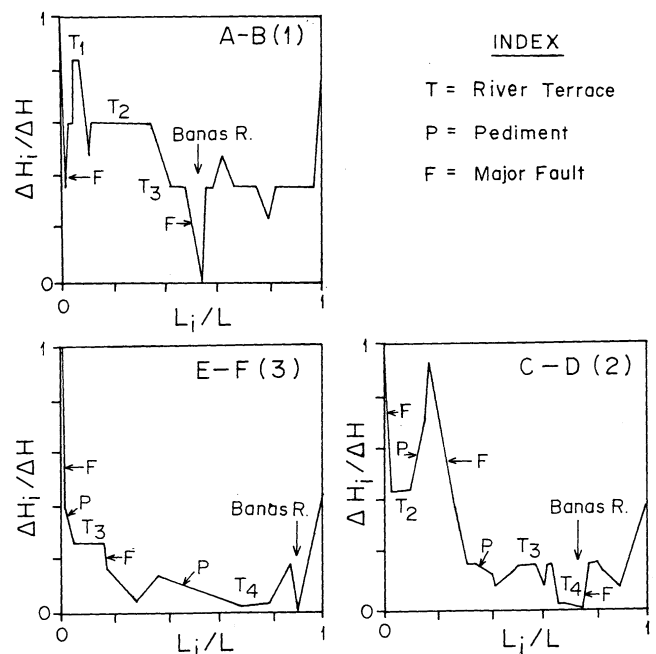


Figure 5. Normalized TRP across the Banas drainage basin. Note how the shape of the TRP clearly depicts the geomorphic and tectonic features.

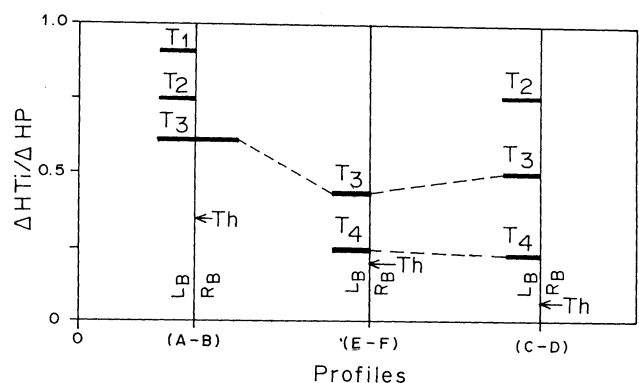


Figure 6. Normalized disposition of the river terraces (T) in the Banas drainage basin in each TRP with respect to the respective thalwegs (Th). L_B , Left bank; R_B , Right bank. Note that except for T_3 in the upper reaches TRP: $A-B$ all the terrace sets in the study sections across the Banas drainage basin are asymmetric, a feature related to the asymmetric nature of the Banas drainage basin, caused by catchment capture. For explanation see the text.

From the TRP parameters and terrace/pediment dispositions, the following general conclusions are made.

The segment of the Banas drainage basin in the central part (TRP: E-F) is more eroded than the segments in the upper and the lower reaches (TRPs: A-B, C-D), because the values of Ea and $Eh * \lambda_n$ are higher in the former segment than in the latter. The TRP: E-F, bisecting the drainage basin into two almost equal parts, shows the maximum basin and valley asymmetries. Interestingly, the highest basin asymmetry is shown by this TRP having the highest valley asymmetry. This feature is likely to have been caused by catchment capture, river piracy and active faulting¹⁰.

High erosion in the central segment of the basin is due to the incision by both the main Banas river and its 5th and 4th order tributaries (e.g. Kothari, Khari, Dai, etc.). This feature is probably related to neotectonically-controlled grade adjustments consequent upon subsidence of the area around the confluence of the Banas river with the Chambal river, as a result of reactivation of the Great Boundary Fault (Figure 7). From the longitudinal profile

characteristics, particularly the knickpoints, of the Banas river and its major tributaries, several horst-graben structures and neotectonically active blocks have been identified¹⁵. These blocks are bounded by reactivated old dislocation zones and active recent faults recording differential vertical movement. Further evidence of neotectonic movement in the area is provided by ponded and disorganized streams¹⁶, and also by the hypsometry of the Banas drainage basin¹⁷.

The normalized longitudinal profile of the Banas river indicates that the maximum concavity of the profile is located fairly upstream¹⁵ (ca. 130 km downstream the source) between TRPs: A-B and E-F. The upstream migration of longitudinal profile concavity is a measure of the river grading⁴, and it indicates that the Banas is a moderately mature river. Therefore, the low-values of Ea and $Eh * \lambda_n$ (40.17 and 0.141, respectively) for the upstream TRP: A-B, indicating poor valley erosion, is understandable, but low to moderate values of these parameters (55.17 and 0.244, respectively) for the downstream TRP: C-D need an explanation. It is likely that this is due

Table 1. Computed parameters of the TRPs across the Banas drainage basin, Rajasthan

Profile	Ea (%)	Eh (L _B)	Eh (R _B)	Eh (L _B)/ Ch	Eh (R _B)/ Ch	Eh^*	$Eh * \lambda_n$	Bs	Vs (degrees)		Va (degrees)
									L _B	R _B	
A-B	40.17	0.35	0.42	0.44	0.52	0.38	0.141	0.05	22	27	5
C-D	55.17	0.59	0.25	1.13	0.48	0.42	0.244	0.15	55	45	10
E-F	75.86	0.70	0.25	1.45	0.52	0.47	0.220	0.42	68	17	51

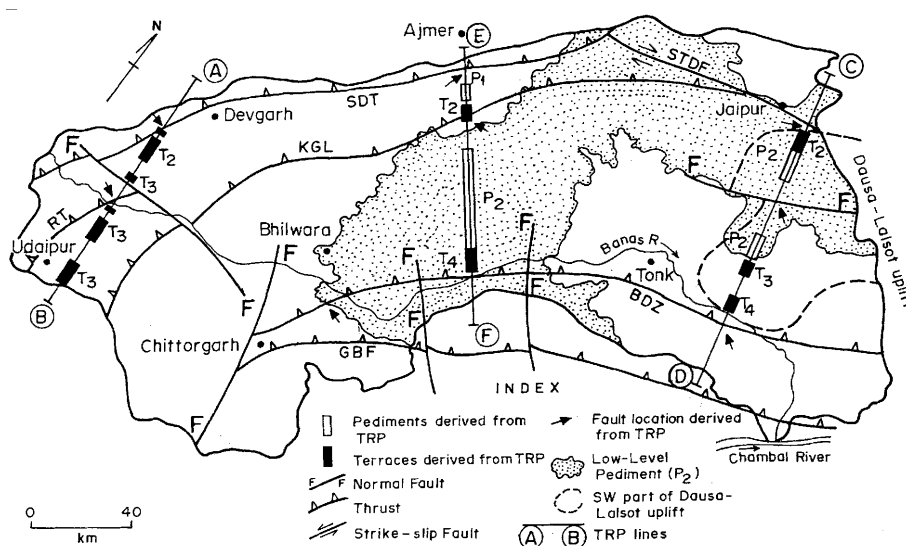


Figure 7. Generalized tectonic map (modified after refs 19 and 20) of the Banas drainage basin showing neotectonically active old and young faults and the position of the river terraces (T) and the pediments (P), identified from TRP analysis. BDZ, Banas Dislocation Zone; GBF, Great Boundary Fault; KGL, Kaliguman Lineament; RT, Rakhabdev Thrust; SDT, South Delhi Thrust; SJDF, Sambhar-Jaipur-Dausa Fault; F-F, Young fault. Note the general correspondence of the fault traces and the pediment surface on the geological map with those identified from TRP analysis.

to neotectonic uplift of the downstream basin segment which is an extension of the 'Dausa uplift'¹⁸.

Eh/Ch ratios (Table 1) for the Banas drainage basin is instructive. On the left bank valley side, the ratio is maximum (1.45 to 1.39) in the middle reach where the major 5th and 4th order tributaries flow, and pedimentation is also prominent (see later in the text). The ratios for the right bank valley side are generally lower than those for the left bank, except for those in the higher reaches. This means that principally the highly active tributaries have carved the landform of the left bank valley side, whereas essentially the main Banas river has eroded the right bank valley side. In the higher reaches, however, the right bank valley side is being more actively eroded than the left bank valley side due to erosion by the 5th order Berach river. TRP: $E-F$ in the middle reaches, showing the maximum Eh/Ch ratio, also shows the maximum basin and valley asymmetries ($Bs = 0.42$, $Va = 51$).

The bedrock resistance and the relative dominance of uplift and river downcutting control the valley side slopes. Ea takes into account both these factors, and thus, is an indicator of the degree of downcutting in response to uplift in neotectonically active domains. The higher the Ea value, more advanced is the erosion and greater is the river maturity in the given TRP location. Logically, an advanced stage of valley-side erosion (higher Ea values), leading to gentler valley side-slopes, would yield highly concave TRP curve for the upper part of the valley sides, with a low convexity for the lower parts⁵. Such types of TRP will also have high Vs values. This is illustrated by the positive correlation between the Ea and Vs values for the left and the right banks of the Banas basin (Figure 8). The misfit point in this diagram pertains to the right bank valley side-slope in the middle reaches, (TRP: $E-F$), where other evidences indicate high terrane subsidence and neotectonically controlled Banas catchment capture by the adjoining Mej river system of the Chambal drainage basin¹⁵.

Four sets of fluvial terraces within an altitude range of 80 to 950 m and two pediplains at 600 m and 350–300 m have been reported from the SW part of the Banas basin¹⁹. The present study using the proposed new method of TRP analysis has also identified four river terrace sets (Figure 6). The oldest and the highest terrace set (T_1) at ca. 800 m is recognized only in the upper reaches (TRP: $A-B$). The next lower and younger terrace set (T_2) occurs at ca. 700 m in the upper reaches and at ca. 500 m in the lower (TRP: $C-D$). T_1 and T_2 terraces are missing in the middle reaches (TRP: $E-F$). It is likely that pedimentation common in the latter reaches has destroyed these high-level terraces. Generally, T_3 is the most extensive terrace set occurring all along the basin, and it has a slope towards NE, i.e. downstream, such that its height decreases from ca. 600 m in the upper reaches to ca. 300 m in the lower reaches. The lowest and the youngest level terrace set (T_4) has not been recognized in the upper reaches where its

near equivalent elevation is occupied by the present Banas river channel. T_4 has also north-easterly downstream slope with the height decreasing from ca. 400 m in the middle reaches to ca. 250 m in the lower reaches. Evidently, the correlation of these terraces is difficult if their heights from the msl are used, because the reconstructed regional terrace surfaces have variable downstream slopes. The problem can be solved, as enumerated earlier in the paper, by normalizing the terrace elevations against the elevation of the main river channel (Figure 6).

The terrace correlation based on elevation on normalized TRP (Figure 6) suggests that the highest level terrace in the lower reaches TRP: $C-D$ can be correlated with T_2 of the higher reaches TRP: $A-B$ rather than with T_3 of the adjacent middle reaches TRP: $E-F$. The levels of the terrace sequence in the lower reaches TRP: $C-D$ are also noteworthy because the terraces here occur at relatively higher elevations from the thalweg than those in other TRPs from their respective thalwegs. This indicates either post-terrace uplift or base-level change/tectonics-induced high incision of a part of the lower reaches of the basin, where the Banas river shows a strong antecedence. An evidence for the latter feature is given by the cross-cut of the Vindhyan hills by the Banas river joining the Chambal river near Khandar. A comparison of the terrace elevations from the respective thalwegs suggests that the area in the lower reaches covered by TRP: $C-D$ has been uplifted 10–35 m between T_3 time and the present, during which period the Banas river has incised as much extra depth in this part of the lower reaches compared to the adjacent middle reaches.

Figure 7 shows the spatial distribution of the terraces and the major pediments on the TRP lines with respect to old, but neotectonically active dislocation and fault zones in the Banas drainage basin. Notably, the fault traces recognized from TRP curves (Figure 5) match well with those geologically mapped and intersected by the TRPs (Figure 7). The high-level pediment surface (P_1) at 550–

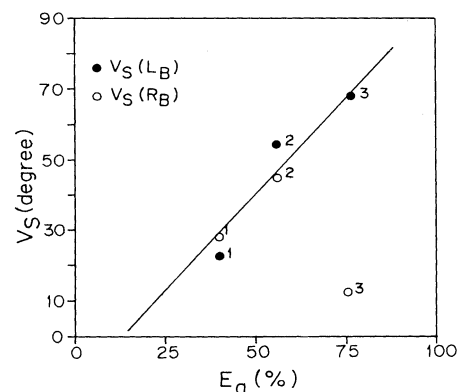


Figure 8. Relation between valley symmetry (Vs) and valley erosion (Ea). 1, TRP: $A-B$; 2, TRP: $C-D$; 3, TRP: $E-F$; LB, Left bank; RB, Right bank. For explanation see the text.

480 m is located in the middle part of the basin at the foot of the Aravalli hill range, and it is best developed in areas to the S and SE of Ajmer. A low-level pediment (P_2) at 420–300 m is an extensive surface, developed in the middle and lower reaches of the basin (Figure 7). This pediment surface is known as the Eastern Banas Plain or the Mewar plateau^{19,20}.

One of the important aspects making the proposed TRP analysis useful is that it is capable of locating structural and geomorphic features from the TRP shape that accentuates the slope breaks, a geomorphic criterion to recognize these features more effectively than the conventional TRPs. This fact is substantiated by the demonstration here that the faults and pediments deduced from TRP study generally correspond to those actually mapped using other methods (Figure 7). The pediments, particularly P_2 , have been dissected by the Banas drainage system, and from the disposition of the terraces it is presumed that the maximum dissection took place during T_3 and T_4 terracing stages. P_2 also shows fluvial terracing, and at places, the pediment grades towards the terrace at its base. Since the pediment has almost a similar height as the river terrace, the former can be temporally related to the latter. The pediment and the terrace may be considered as a pair⁸, and hence, synchronous morphologic features.

The new approach to the analysis of the TRPs, enumerated here, can find application in both inter-profile and inter-drainage basin comparisons of morphotectonic features. The case study in the Banas drainage basin, Rajasthan, has demonstrated that significant inferences on neotectonics and river valley erosion can be extracted from the quantified transverse river valley profile parameters.

3. Bull, W. B. and Knuepfer, P. L. K., *Geomorphology*, 1987, **1**, 15–32.
4. Demoulin, A., *Geomorphology*, 1998, **24**, 189–208.
5. Leopold, L. B., Wolman, M. C. and Miller J. P., *Fluvial Processes in Geomorphology*, W.H. Freeman & Co., London, 1964, pp. 7–522.
6. Vaidyanadhan, R., *Indian J. Earth Sci.*, 1977, S. Ray volume, 13–35.
7. Sinha-Roy, S., in *Geographic Mosaic* (ed. Mukhopadhyay, S. C.), Manasi Press, Calcutta, 1985, pp. 88–124.
8. Plakht, J. P., Patyk-Kara, N. and Gorelinkva, N., *Earth Sur. Process Landforms*, 2000, **25**, 29–39.
9. Bloom, A. L., *Geomorphology*, Prentice-Hall Pvt Ltd, New Delhi, 1979, pp. 1–150.
10. Sinha-Roy, S., *Curr. Sci.*, 2001, **80**, 293–298.
11. Hack, J. T. and Goodlett, J. C., *US Geol. Surv. Prof. Pap.*, 1960, **347**, 1–66.
12. Melton, M. A., *Bull. Geol. Soc. Am.*, 1960, **71**, 133–144.
13. Bull, W. B. and McFadden, J. D., in *Geomorphology in Arid Regions* (ed. Doehring, D. O.), Allen and Unwin, London, 1980, pp.115–138.
14. Fry, J. C. and Leonard, A. R., *Am. J. Sci.*, 1954, **253**, 242–251.
15. Sinha-Roy, S., *J. Geol. Soc. India*, 2001 (in press).
16. Roy, A. B., *Curr. Sci.*, 1999, **76**, 290–295.
17. Sinha-Roy, S., *J. Geol. Soc. India*, 2001 (in press).
18. Singh, S. P., *Rec. Geol. Surv. India*, 1982, **112**, 46–62.
19. Gupta, S. N., Arora, Y. K., Mathur, R. K., Iqbaluddin, Prasad, B., Sahai, T. N. and Sharma, S. B., *Mem. Geol. Surv. India*, **123**, 1–262.
20. Sinha-Roy, S., Malhotra, G. and Mohanty, M., *Geology of Rajasthan*, Geol. Soc. India, Bangalore, 1998, pp. 1–278.

ACKNOWLEDGEMENTS. This study forms a part of a project financially supported by the Ministry of Environment and Forests, Government of India, New Delhi. Shri Suneet Sethi has helped in data computation. I thank Dr P. Ghosh, Executive Director, Birla Institute of Scientific Research, Jaipur, for providing facilities for this study. I thank the anonymous referee for useful comments.

1. Hack, J. T., *J. Res. US Geol. Surv.*, 1973, **1**, 421–429.
2. Seeber, L. and Gornitz, V. M., *Tectonophysics*, 1983, **92**, 335–367.

Received 18 September 2000; revised accepted 29 March 2001